ITERATIVE EM CHANNEL ESTIMATION FOR TURBO-CODED DS CDMA RECEIVER UNDER DIFFERENT COMMUNICATION SCENARIOS

A Thesis by

Neelu Bijukchhe

B.E., Nepal Engineering College, Pokhara University, Nepal, 2004

Submitted to the Department of Electrical and Computer Engineering
and the faculty of the Graduate School of
Wichita State University
in partial fulfillment of
the requirements for the degree of
Master of Science

May 2008

ITERATIVE EM CHANNEL ESTIMATION FOR TURBO-CODED DS CDMA RECEIVER UNDER DIFFERENT COMMUNICATION SCENARIOS

The following faculty have examined the final copy of this thesis for form and content, and recommend that it be accepted in partial fulfillment of the requirement for the degree of Master of Science with a major in Electrical Engineering.

_____
Hyuck M. Kwon, Committee Chair

_____
Kamesh R. Namuduri, Committee Member

_____
Alexandre Boukhgueim, Committee Member

DEDICATION

To my parents

Anyone who has never made a mistake has never tried anything new.
-Albert Einstein

ACKNOWLEDGEMENTS

I would like to thank the faculty and staff of the Department of Electrical and Computer Engineering at Wichita State University. It is my privilege to thank Dr. Hyuck M. Kwon for his patience and guidance provided throughout the process. I also thank Dr. Don Torrieri for his suggestions that have been useful for this thesis. I am grateful to my committee members, Dr. Namuduri and Dr. Boukhgueim, for their support. I express my appreciation to my colleagues in the Wireless Research and Development Group (WiReD); in particular I would like to thank Amitav for his great help and encouragement. I also thank my friends and roommates, who have been my greatest support and encouragement. Finally, I thank my family for their enduring love and support.

ABSTRACT

This thesis proposes a scheme of iteratively obtaining an estimate of channel coefficients and noise power spectral density (PSD) using expectation maximization for a turbo-coded code division multiple-access (CDMA) receiver. The expectation maximization (EM) channel estimation is tested under different communication scenarios such as time-varying interference and pulse-band jamming. For time-varying interference and pulse-band jamming scenarios, the initial estimate of channel coefficient and the noise PSD are obtained from pilot symbols. Further estimations of channel coefficient and noise PSD are refined using turbo decoder soft outputs. The proposed systems are verified through simulations using a structure similar to the Third Generation Partnership Project Long-Term Evolution (3GPP LTE) system under Jakes and Rayleigh fading environments.

In addition, this thesis proposes the scheme of obtaining an estimate of channel coefficients and noise PSD without sending any pilots under a single-user environment. At the receiver, the initial estimate of channel coefficient and noise PSD are obtained without pilots using blind estimation, and then the further estimations are done using EM. The estimated values are updated iteratively by feedback from the turbo decoder. The elimination of pilot symbols sacrifices performance but allows increased energy per transmitted symbol, increased information throughput, or the inclusion of additional parity bits.

TABLE OF CONTENTS

LIST OF FIGURES

LIST OF FIGURES (continued)

LIST OF ABREVIATIONS

3GPP	Third Generation Partnership Project
AWGN	Additive White Gaussian Noise
BER	Bit Error Rate
BPSK	Binary Phase-Shift Keying
CDMA	Code Division Multiple Access
EM	Expectation Maximization
LDPC	Low Density Parity Check
MAP	Maximum a Posteriori
ML	Maximum Likelihood
PBNJ	Partial Band Noise Jamming
PSD	Power Spectral Density
RSC	Recursive Systematic Convolutional
SNR	Signal-to-Noise Ratio

LIST OF SYMBOLS

α	Alpha
β	Beta
γ	Gamma
ϕ	Phi
θ	Theta

CHAPTER 1

INTRODUCTION

1.1 Motivation

In conventional receivers, signal-to-noise ratio (SNR) is determined by measuring received signal strength at the receiver front end by assuming a constant noise power spectral density (PSD). In practice, noise PSD that includes multiple access and partial-band jamming varies with time.

The iterative receiver concept was demonstrated by Torrieri et al. in [1]-[5]. In iterative receiver, both channel coefficient and noise PSD were iteratively estimated by feeding back the decoder soft outputs. The study of iterative EM estimation and turbo coding along with assumption of non-coherent frequency shift-keying modulation and demodulation was demonstrated in [1]. Also the study of an iterative code-division multiple-access (CDMA) receiver with EM channel estimation and turbo decoding was demonstrated in [2]. In [3]-[5], an iterative receiver with EM channel estimation and low-density parity-check (LDPC) codes was studied under single-user environment, time-varying interference and M-ary modulation respectively.

In addition, studies by Torrieri et al. [2]-[5] were based on the use of pilot-symbol-aided modulation (PSAM) for the initial channel estimation. In previous papers [1] and [2], the iterative turbo-coded receiver was not tested under different communication scenarios such as time-varying interference and partial-band jamming.

1.2 Objectives

One objective of this thesis is to evaluate the iterative turbo-coded receiver under different communication scenarios such as time-varying interference and partial-band jamming.

The proposed time-varying PSD estimation scheme is expected to show significant gains over a conventional model with non-adaptive PSD. Another objective of this thesis is to present the scheme of obtaining an estimate of channel coefficients and noise PSD without sending any pilots using the iterative EM turbo-coded receiver. The elimination of pilot symbols allows an increased energy per transmitted symbol, an increased information throughput, or the inclusion of additional parity bits. Finally, this thesis explains the testing of realistic communication scenarios and shows the simulation results.

1.3 Contributions

This thesis made the following contributions:

- Evaluated the iterative EM turbo-coded receiver under realistic multi-user environment such as a time-varying interference plus noise PSD.
- Evaluated the iterative EM turbo-coded receiver under pulse band jamming case.
- Conducted extensive search for the best pilot fraction.
- Developed an iterative EM turbo-coded receiver for the no-pilots case.
- Evaluated the iterative receiver without any pilots by using increased energy per symbol.

1.4 Thesis Organization

This thesis is organized as follows: Chapter 2 describes the system model including slot structure and channel. Chapter 3 presents the proposed EM-based iterative turbo-coded receiver including pilot and no-pilot cases. Chapter 4 presents the communication scenarios considered for testing the proposed receiver. Chapter 5 shows simulation results, and Chapter 6 draws conclusions.

CHAPTER 2

SYSTEM MODEL

2.1 Transmitter

Figure 1 shows a transmitter model. Information bits are applied to a turbo encoder that produces the code bits [6]. After the channel interleaving, the code bits are combined with a spreading sequence and then modulated using binary phase-shift keying (BPSK). Each spreading sequence is an orthogonal variable-length spreading factor (OVSF) sequence with a chip rate of 1.28 Mcps. The OVSF allows multiple users to access and share communication links [7]-[9].

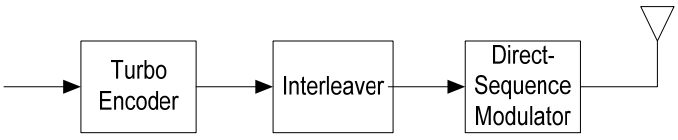

Figure 1. Transmitter structure.

As in the Third Generation Partnership Project (3GPP) system, a frame with 10-ms duration consists of two subframes, each with seven slots. In this thesis, a new slot structure without pilots is also considered.

2.2 Slot Structure

Slot Structure with Pilot Case

Figure 2 shows an example of a slot structure consisting of two data parts, one midamble part, and one guard period as in the previous work [2]. The data-modulated OVSF spreading sequences are located in the data parts, pilot chips are located in the midamble part for estimation of channel coefficient, C, and noise PSD, N_0, and no signal is placed in the guard period (GP) to avoid inter-symbol interference in the next slot due to multipath signals.

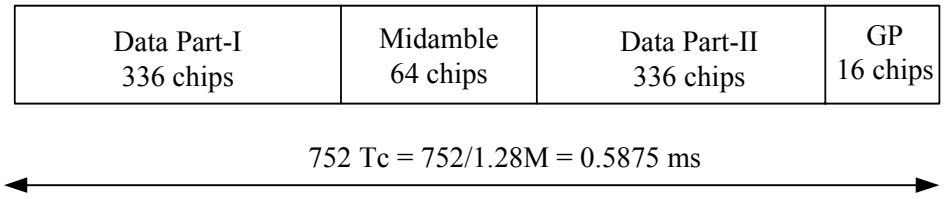

Figure 2. Slot structure with midamble pilot chips, T_c = chip duration.

Slot Structure with No-Pilot Case

Figure 3 shows a new slot structure which consists of a data part and guard period only, i.e.; without any pilots.

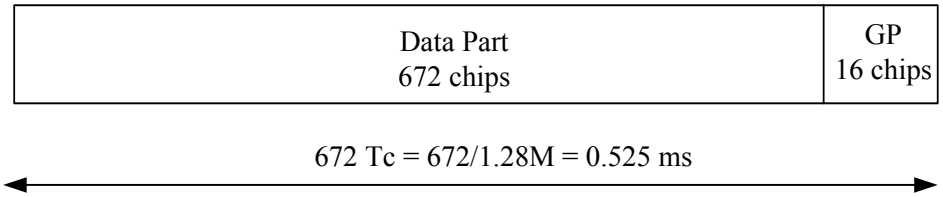

Figure 3. Slot structure without midamble pilot chips.

Assume that a user is assigned a single slot out of seven slots in a subframe, a *spreading factor* (SF) of 8, a turbo code rate of 1/3, and a total of 672 chips for two data parts per slot. Then, using 20 non-consecutive slots in ten frame intervals, the user can transmit a block of β = 560 information bits because each slot can carry 672/SF = 84 code bits, i.e., 84/3 = 28 information bits. A turbo codeword consists of 3β coded bits.

2.3 Channel Model

Signals are transmitted through Jakes flat-fading (i.e., correlated fading) and Rayleigh fading channels (i.e., independent fading), and complex additive white Gaussian noise (AWGN) is added to the received signal. Block fading is considered in the scenarios of time-varying interference and no-pilots case. AWGN is considered in the partial-band jamming case. During a fading block interval n_{FB}, the fading coefficient C and the noise PSD N_0 are assumed to be

constant unknown variables. A mobile speed of v = 3 km/h is used for the Jakes fading model, assuming a carrier frequency of f_c = 2 GHz. In addition, the slot structure shown in Figure 3 is used in a single user environment.

CHAPTER 3

ITERATIVE TURBO CODED RECEIVER

3.1 Turbo Encoder

Figure 4 depicts a rate-1/3 turbo encoder [1]-[2] that includes two identical recursive systematic convolutional (RSC) encoders with constraint-length equal to 4. The generator polynomial of each RSC encoder is **g** = [1101, 1011]. The first component 1101 of **g** is the feed-forward connections for generation of coded bit $d_{t,2}$, and the second component 1011 is the feed-back connections for the recursion in the encoder. The output bit $d_{t,1}$ is a systematic code bit equal to information bit d_t, where the subscript t denotes the information-bit index. The output bits ($d_{t,2}$, $d_{t,3}$) are the parity code bits.

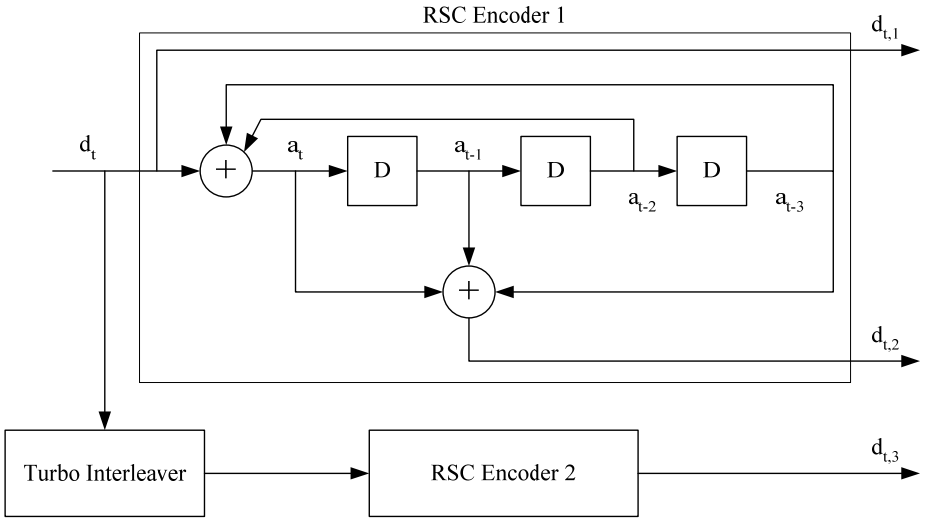

Figure 4. Turbo encoder with two RSC encoders.

3.2 Iterative Receiver Structure

Figure 5 is a block diagram of the proposed iterative receiver. After despreading, the received signal input to the demodulator and channel estimator is [10]

$$y_k = C \cdot x_k + n_k, \quad k = 1, 2, \ldots, 3\beta \tag{1}$$

where the subscript k denotes the code-bit index, 3β = the turbo codeword length, n_k = complex Gaussian noise with $E[|n_k|^2] = N_0$, and $x_k = +1$ or -1.

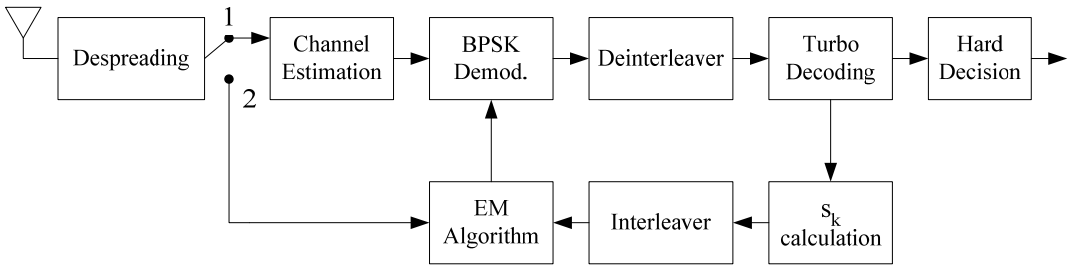

Figure 5. Proposed iterative receiver.

The channel estimator produces estimates $\left(\hat{C}, \hat{N}_0\right)$ that are sent to the demodulator, which computes the metric $4\hat{C}y_k / \hat{N}_0$ and sends it to the turbo decoder. Each turbo component decoder then uses a *maximum a posteriori* rule to decode the data bits. Let $\boldsymbol{y}$ denote a component decoder's received signal vector of dimension (3β × 1). The component decoder computes the log-likelihood ratio:

$$\Lambda(d_t) = \log \frac{\Pr\{d_t = 1 \mid \boldsymbol{y}\}}{\Pr\{d_t = 0 \mid \boldsymbol{y}\}}, \quad 1 \le t \le \beta \tag{2}$$

These decoder outputs are fed back to the channel estimator to enable it to generate estimates of the fading coefficient and noise PSD iteratively. Initially, prior to the decoder producing an output, the channel estimates are obtained by averaging over the pilot symbols in the *midamble* part of a slot, which are all equal to +1 in the absence of noise.

Three iteration indices are used throughout this thesis:

j denotes the index for the receiver iteration, $j = 1,\ldots,(j_{\max} = 9)$. Up to 9 receiver iterations are considered as it was shown by Torrieri et al. in [3] that there is minimal performance improvement beyond 9 receiver iterations.

q denotes the index for the EM iteration, $q = 1,\ldots,(q_{\max} = 3)$. The number of EM iterations is identical to [2].

l denotes the index for the internal turbo decoder iterations, $l = 1,\ldots,(l_{\max} = 3)$ as in [2] for comparative purposes.

The flowchart representation of the iterative receiver structure in Figure 6 offers clearer insight into the various iterations. The iterative receiver is initiated by channel estimates obtained from pilot symbols at j = 1. These initial estimates are used for the first demodulation and decoding, which provides the first set of s_k values that are passed to the EM estimator. These s_k values are used to calculate $R_{k,(j)}^{(q)}$ and $\overline{x}_{k,(j)}^{(q)}$, respectively for the q^{th} EM iteration from equations (21) and (19). Using $\overline{x}_{k,(j)}^{(q)}$ and $R_{k,(j)}^{(q)}$ from the previous receiver iteration and using equations (16) and (17), $C_{(j+1)}^{(q)}$ and $N_{0,(j+1)}^{(q)}$ are calculated, which in turn are passed to equations (19) and (21) to provide better values of $\overline{x}_{k,(j+1)}^{(q)}$ and $R_{k,(j+1)}$ which establishes the EM iteration. The improved values of $\overline{x}_{k,(j+1)}^{(q)}$ and $R_{k,(j+1)}^{(q)}$ are again used to calculate refined $C_{(j+1)}^{(q+1)}$ and $N_{0,(j+1)}^{(q+1)}$ where q = 1,…,3, using equations (16) and (17).This loop is executed until it reaches $q_{\max}$= 3, thus providing $C_{(j+1)}^{(q+1)}$ and $N_{0,(j+1)}^{(q+1)}$. Now the outermost receiver iteration is increased to j+1 and the process continues.

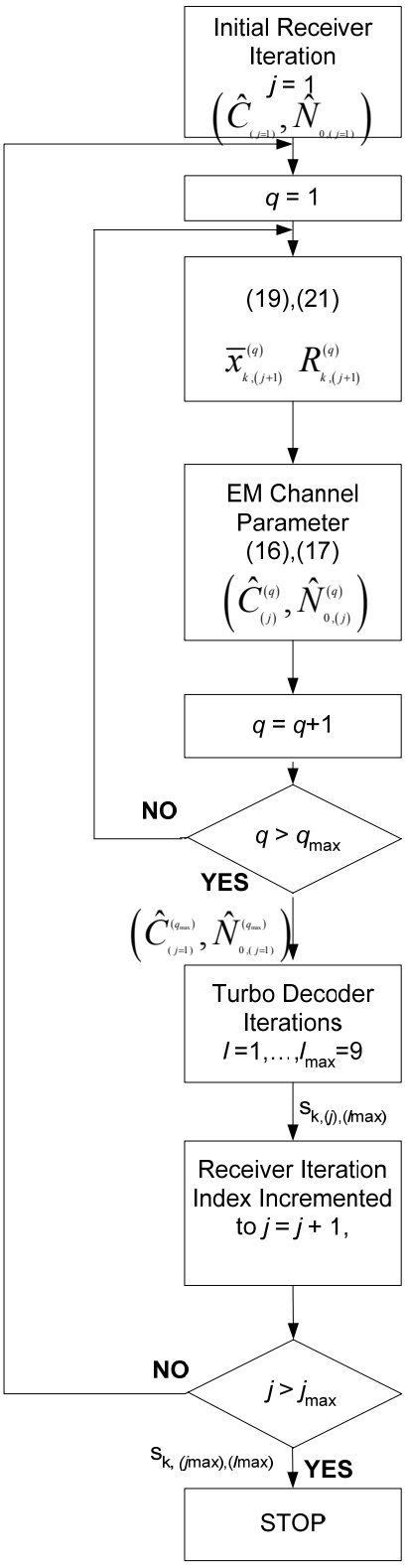

Figure 6. Flow chart showing iterative receiver structure.

3.3 Iterative Receiver Without pilots

In order to eliminate pilot symbols, the initial receiver iteration can employ blind estimation to approximate the initial channel amplitude and noise PSD per fading block as,

$$\left|\hat{C}_{(j=1)}\right| = \frac{\left[\left|y_k\right|_{\max} + \left|y_k\right|_{\min}\right]}{2} \tag{3}$$

$$\hat{N}_{0,(j=1)} = \max\left(\left|D - \left(\hat{C}_{(j=1)}\right)^2\right|, f\left(\hat{C}_{(j=1)}\right)^2\right) \tag{4}$$

where $D = \frac{1}{n_{FB}} \sum_{n_{FB}} \left|y_k\right|^2$, and $0 < f \leq 1$, f is a fraction being chosen such that $\hat{C}_{(j=1)} \big/ \hat{N}_{0,(j=1)}$ does not exceed some maximum value and j denotes the receiver iteration index. Ideally, f is a function of SNR, but a constant $f = 0.1$ is used over all SNR values. After the initial iteration, the decoder employs the EM algorithm for further iterations.

Figure 7 shows the plot of parameters considered in equation (4). Here the fading block size is chosen as 752 and f as 0.1 throughout the simulation.

3.4 EM Algorithm

For a given receiver iteration j, the EM algorithm is applied to estimate the complex channel coefficient C and the noise PSD N_0, based on the Maximum Likelihood (ML) criterion. Let $\Theta = (C, N_0)$ denote the two unknown parameters to be estimated iteratively in a fading block with the turbo decoding outputs. The ML estimation is obtained by maximizing the logarithm of a likelihood function of the observation vector $\boldsymbol{y}$, called an *incomplete* data vector, as

$$\hat{\Theta} = \arg\max_{\Theta} \ln f(\boldsymbol{y} \mid \Theta) \tag{5}$$

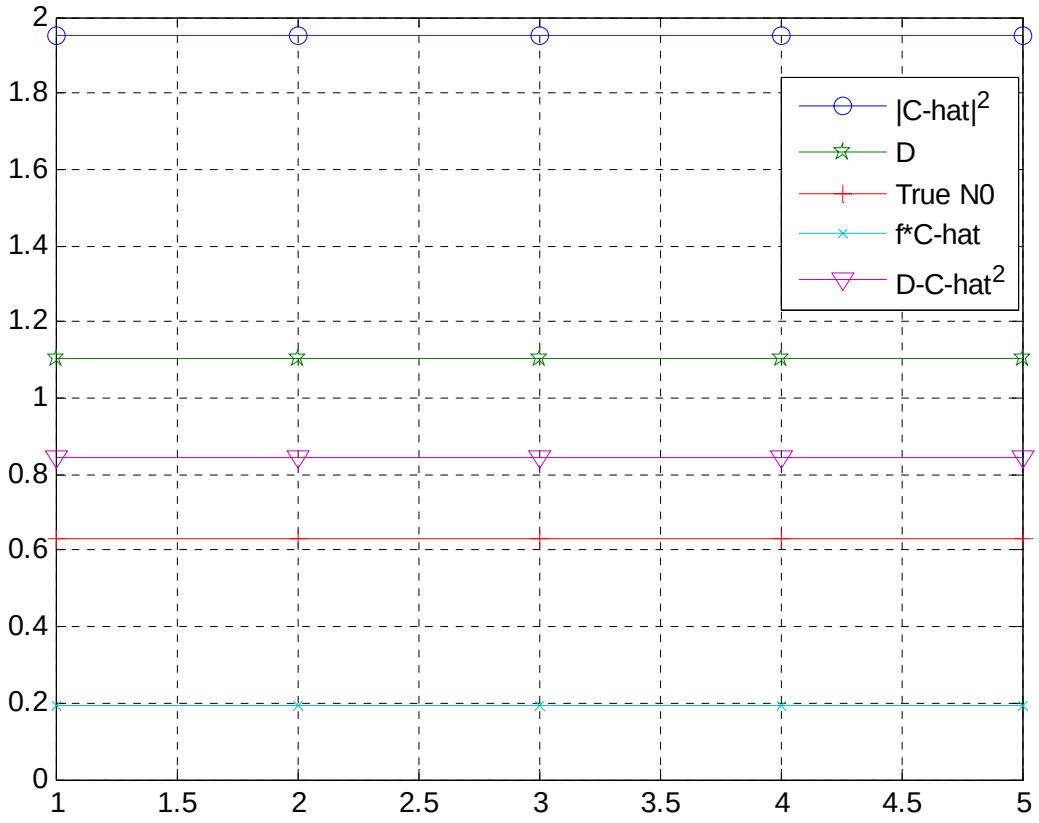

Figure 7. Various parameters from (3) and (4), $f = 0.1$.

Since the ML estimation in equation (5) is difficult to compute, another random vector $\boldsymbol{z} = \{\boldsymbol{x}, \boldsymbol{y}\}$, called a *complete* data vector, is considered. Here, the input data vector $\boldsymbol{x}$ denotes the transmitted ($\tau \times 1$) symbol vector, where τ denotes the number of pilot symbols in the midamble during the initial channel estimation. The dimension of $\boldsymbol{y}$ is equal to that of $\boldsymbol{x}$. Since $\boldsymbol{x}$ is independent of Θ, the likelihood function of $\boldsymbol{z}$ is

$$f(\boldsymbol{x}, \boldsymbol{y} \mid \Theta) = f(\boldsymbol{y} \mid \boldsymbol{x}, \Theta) \cdot f(\boldsymbol{x} \mid \Theta) = f(\boldsymbol{y} \mid \boldsymbol{x}, \Theta) \cdot f(\boldsymbol{x}). \tag{6}$$

The EM algorithm finds the value of Θ that maximizes the function

$$Q\left(\Theta \mid \Theta_{(j)}^{(q)}\right) \square E_{\boldsymbol{x}|\boldsymbol{y},\Theta^{q}}\left[\ln f\left(\boldsymbol{x}, \boldsymbol{y} \mid \Theta\right)\right] = \int \ln f\left(\boldsymbol{x}, \boldsymbol{y} \mid \Theta\right) \cdot f\left(\boldsymbol{x} \mid \boldsymbol{y}, \Theta_{(j)}^{(q)}\right) d\boldsymbol{x} \tag{7}$$

where $\Theta_{(j)}^{(q)}$ is the parameter estimate for the q^{th} EM iteration at the j^{th} receiver iteration, i.e., $\Theta_{(j)}^{(q)} = \left(C_{(j)}^{(q)}, N_{(j)}^{(q)}\right)$. Since $f(\boldsymbol{x})$ has no dependence on Θ, it can be dropped in the maximization, and the substitution of (6) into (7) gives

$$Q\left(\Theta \mid \Theta_{(j)}^{(q)}\right) = \int \ln f\left(\boldsymbol{y} \mid \boldsymbol{x}, \Theta\right) \cdot f\left(\boldsymbol{x} \mid \boldsymbol{y}, \Theta_{(j)}^{(q)}\right) d\boldsymbol{x} \,. \tag{8}$$

Expectation Step: The vector likelihood function $f\left(\boldsymbol{y} \mid \boldsymbol{x}, \Theta\right)$ in (8) is a product of the k-th symbol likelihood functions: $f(y_k \mid x_k, \Theta)$, k = 1, 2, ... , τ=3β. Given the values of x_k and Θ, y_k is a circularly symmetric, complex Gaussian random variable given by [11]

$$f\left(y_k \mid x_k, \Theta\right) = \frac{1}{\pi \cdot N_0} \exp\left(-\frac{|\, y_k - C \cdot x_k \,|^2}{N_0}\right) = \frac{1}{\pi \cdot N_0} \exp\left(-\frac{|\, y_k \,|^2 + |\, C \,|^2 - 2 \cdot \mathrm{Re}\left\{y_k^* \cdot C \cdot x_k\right\}}{N_0}\right) \tag{9}$$

where the superscript * denotes the conjugate, C is a block fading coefficient, $\left|x_k\right|^2 = 1$ since BPSK is used, and k = 1, …, τ=3β. Substituting equation (9) into (8), we obtain

$$Q\left(\Theta \mid \Theta_{(j)}^{(q)}\right) = \iint\limits_{k=1,..,\tau} \left[-\tau \ln\left(\pi N_0\right) - \frac{1}{N_0} \sum_{k'=1}^{\tau} |\, y_{k'} \,|^2 + |\, C \,|^2 - 2\,\mathrm{Re}\left\{y_{k'}^* C \overline{x}_{k',(j)}^{(q)}\right\}\right] \prod_{k=1}^{\tau} f\left(x_k \mid y_k, \Theta_{(j)}^{(q)}\right) dx_k. \tag{10}$$

The integration over the $2\,\mathrm{Re}\left\{y_{k'}^* C x_{k',(j)}^{(q)}\right\}$ term can be simplified as

$$\begin{aligned} \sum_{k'=1}^{\tau} \iint\limits_{k=1,..,\tau} \mathrm{Re}\left\{y_{k'}^* C x_{k',(j)}^{(q)}\right\} \prod_{k=1}^{\tau} f\left(x_k \mid y_k, \Theta_{(j)}^{(q)}\right) dx_k &= \sum_{k'=1}^{\tau} \mathrm{Re}\left\{y_{k'}^* C\right\} \iint\limits_{k=1,..,\tau} x_{k',(j)}^{(q)} \prod_{k=1}^{\tau} f\left(x_{k,(j)}^{(q)} \mid y_k, \Theta_{(j)}^{(q)}\right) dx_k \\ &= \sum_{k'=1}^{\tau} \mathrm{Re}\left\{y_{k'}^* C\right\} \; \overline{x}_{k',(j)}^{(q)} \end{aligned} \tag{11}$$

since all the integrals of probability density functions are equal to 1 for $k \neq k'$, and

$$\overline{x}_{k,(j)}^{(q)} = \int x_{k,(j)}^{(q)} f\left(x_{k,(j)}^{(q)} \mid y_k, \Theta_{(j)}^{(q)}\right) dx_k \quad k = k' \tag{12}$$

Therefore,

$$Q\left(\Theta \mid \Theta_{(j)}^{(q)}\right) = E\left[\ln\left(f(\boldsymbol{x},\boldsymbol{y} \mid \Theta)\right)\right] = -\tau \ln\left(\pi N_0\right) - \frac{1}{N_0}\sum_{k=1}^{\tau}\left(|\, y_k \,|^2 + |\, C \,|^2 - 2\,\mathrm{Re}\left\{y_k^* C\right\}\overline{x}_{k,(j)}^{(q)}\right). \quad (13)$$

Maximization Step: To find the optimum parameters that maximize the expectation, we take derivatives of equation (13) with respect to C and N_0, respectively, and set them to zero as

$$\frac{dQ\left(\Theta \mid \Theta_{(j)}^{(q)}\right)}{dC} = -\frac{1}{N_0}\sum_{k=1}^{\tau}\left(C^* + y_k^*\overline{x}_{k,(j)}^{(q)}\right) = 0 \quad (14)$$

and

$$\frac{dQ\left(\Theta \mid \Theta_{(j)}^{(q)}\right)}{dN_0} = -\frac{\tau}{N_0} + \frac{1}{N_0^2}\sum_{k=1}^{\tau}\left(|\, y_k \,|^2 + |\, C \,|^2 - 2\,\mathrm{Re}\left\{y_k^* C\right\}\overline{x}_{k,(j)}^{(q)}\right) = 0\,. \quad (15)$$

The optimum parameters can be found from (14) and (15), respectively, as

$$\hat{C}_{(j)}^{(q)} = \frac{1}{\tau}\sum_{k=1}^{\tau} y_k \overline{x}_{k,(j)}^{(q)} \quad (16)$$

and

$$\hat{N}_{0,(j)}^{(q)} = \frac{1}{\tau}\sum_{k=1}^{\tau}\left(|\, y_k \,|^2 + |\, \hat{C}_{(j)}^{(q)} \,|^2 - 2\,\mathrm{Re}\left\{y_k^* \hat{C}_{(j)}^{(q)}\right\}\overline{x}_{k,(j)}^{(q)}\right). \quad (17)$$

Both of these equations require the value of $\overline{x}_{k,(j)}^{(q)}$ in (12), which can be expanded as

$$\begin{aligned}\overline{x}_{k,(j)}^{(q)} &= (x_k = 1)\cdot f\left(x_k = 1 \mid y_k, \Theta_{(j)}^{(q)}\right) + (x_k = -1)\cdot f\left(x_k = -1 \mid y_k, \Theta_{(j)}^{(q)}\right) \\ &= f\left(x_k = 1 \mid y_k, \Theta_{(j)}^{(q)}\right) - f\left(x_k = -1 \mid y_k, \Theta_{(j)}^{(q)}\right). \end{aligned} \quad (18)$$

An evaluation of this equation gives

$$\overline{x}_{k,(j)}^{(q)} = \Pr(x_k = 1)\cdot\frac{f\left(y_k \mid x_k = 1, \Theta_{(j)}^{(q)}\right)}{f\left(y_k \mid \Theta_{(j)}^{(q)}\right)} - \Pr(x_k = -1)\cdot\frac{f\left(y_k \mid x_k = -1, \Theta_{(j)}^{(q)}\right)}{f\left(y_k \mid \Theta_{(j)}^{(q)}\right)}$$

$$= \frac{(1-s_{k,(j)}) f\left(y_k \mid x_k = 1, \Theta_{(j)}^{(q)}\right) - s_k f\left(y_k \mid x_k = -1, \Theta_{(j)}^{(q)}\right)}{(1-s_{k,(j)}) f\left(y_k \mid x_k = 1, \Theta_{(j)}^{(q)}\right) + s_k f\left(y_k \mid x_k = -1, \Theta_{(j)}^{(q)}\right)} = \frac{(1-s_{k,(j)}) - s_{k,(j)} \dfrac{f\left(y_k \mid x_k = -1, \Theta_{(j)}^{(q)}\right)}{f\left(y_k \mid x_k = 1, \Theta_{(j)}^{(q)}\right)}}{(1-s_{k,(j)}) + s_{k,(j)} \dfrac{f\left(y_k \mid x_k = -1, \Theta_{(j)}^{(q)}\right)}{f\left(y_k \mid x_k = 1, \Theta_{(j)}^{(q)}\right)}}$$

$$= \frac{(1-s_{k,(j)}) - s_{k,(j)} R_{k,(j)}^{(q)}}{(1-s_{k,(j)}) + s_{k,(j)} R_{k,(j)}^{(q)}} \tag{19}$$

where $\Pr\left(x_k \mid \Theta^q\right) = \Pr\left(x_k\right)$ was used in the first equality,

$$s_{k,(j)} \triangleq \Pr\left(x_k = -1\right), \tag{20}$$

and

$$R_{k,(j)}^{(q)} \triangleq \frac{f\left(y_k \mid x_k = -1, \Theta_{(j)}^{(q)}\right)}{f\left(y_k \mid x_k = 1, \Theta_{(j)}^{(q)}\right)} = \frac{1/(\pi N_{0,(j)}^{(q)}) \cdot \exp\left(-\left| y_k - C^q \cdot (x_k = -1)\right|^2 / N_{0,(j)}^{(q)}\right)}{1/(\pi N_{0,(j)}^{(q)}) \cdot \exp\left(-\left| y_k - C^q \cdot (x_k = 1)\right|^2 / N_{0,(j)}^{(q)}\right)}$$

$$= \exp\left(-4\,\mathrm{Re}\left\{\frac{y_k^* C_{(j)}^{(q)}}{N_{0,(j)}^{(q)}}\right\}\right). \tag{21}$$

Equations (16), (17), and (21) provide iterative estimates of $\hat{C}$ and $\hat{N}_0$ in terms of the previous estimates $C_{(j)}^{(q)}$ and $N_{0,(j)}^{(q)}$. If $\Pr\left(d_k = 0 \text{ bit} \middle| \boldsymbol{y}\right)$ is regarded as an approximation of s_k, then (2) implies that

$$s_k = \frac{1}{1 + e^{\Lambda(d_k)}} \tag{22}$$

where $k = t$ for the systematic bit, and $t = k \bmod 3$.

The other two s_k values for the redundant bits at $k = t+1$ and $k = t+2$ can be computed by considering the RSC encoder 1 and 2 structures in Figure 4. From RSC encoder 1,

$$a_t = d_t \oplus a_{t-2} \oplus a_{t-3} \tag{23}$$

and

$$d_{t,2} = a_t \oplus a_{t-1} \oplus a_{t-3} \tag{24}$$

where additions are modulo 2. The a_t and d_t in equations (23) and (24) denote 0 or 1 bits, and d_t, a_t, a_{t-1}, a_{t-2}, and a_{t-3} are independent of each other. Assume zero initial conditions for a_{t-1}, a_{t-2}, and a_{t-3} in the shift register generators, i.e., $\Pr(a_{t-1} = 0) = \Pr(a_{t-2} = 0) = \Pr(a_{t-3} = 0) = 1$ for the initial iteration are assigned. Equation (23) implies that an iterative computation of $\Pr(a_t = 0)$ is

$$\begin{aligned}\Pr(a_t = 0) = {} & \Pr(d_t = 0) \cdot \Pr(a_{t-2} = 0) \cdot \Pr(a_{t-3} = 0) + \Pr(d_t = 0) \cdot \Pr(a_{t-2} = 1) \cdot \Pr(a_{t-3} = 1) \\ & + \Pr(d_t = 1) \cdot \Pr(a_{t-2} = 0) \cdot \Pr(a_{t-3} = 1) + \Pr(d_t = 1) \cdot \Pr(a_{t-2} = 1) \cdot \Pr(a_{t-3} = 0) . \end{aligned} \tag{25}$$

Equation (24) implies that

$$\begin{aligned} s_{t+1} = \Pr(d_{t,2} = 0) = {} & \Pr(a_t = 0) \cdot \Pr(a_{t-1} = 0) \cdot \Pr(a_{t-3} = 0) + \Pr(a_t = 0) \cdot \Pr(a_{t-1} = 1) \cdot \Pr(a_{t-3} = 1) \\ & + \Pr(a_t = 1) \cdot \Pr(a_{t-1} = 0) \cdot \Pr(a_{t-3} = 1) + \Pr(a_t = 1) \cdot \Pr(a_{t-1} = 1) \cdot \Pr(a_{t-3} = 0) \end{aligned} \tag{26}$$

and $s_{t+2} = \Pr(d_{t,3} = 0) = \Pr(x_{t+2} = -1)$ can be calculated similarly. After channel interleaving shown in Figure 6, all s_k values, k = 1, ... , t, t+1, t+2, …, 3 β, are forwarded to the EM algorithm for the next parameter update.

For a given receiver iteration j, $\overline{x}_{k,(j)}^{(q)}$ and $R_{k,(j)}^{(q)}$ are updated q times using soft values of $s_{k,(j)}$, which are sent from the turbo decoder. When a pilot symbol is processed, s_k is set equal to zero for that symbol in that channel estimator. Now the receiver iteration is increased to j+1. Using $\overline{x}_{k,(j)}^{(q)}$ and $R_{k,(j)}^{(q)}$ from the previous receiver iteration and using equations (16) and (17), $C_{(j+1)}^{(q)}$ and $N_{0,(j+1)}^{(q)}$ are calculated, which in turn are passed to equations (19) and (21) to provide better values of $\overline{x}_{k,(j+1)}^{(q)}$ and $R_{k,(j+1)}$. The improved values of $\overline{x}_{k,(j+1)}^{(q)}$ and $R_{k,(j+1)}^{(q)}$ are again used to calculate refined $C_{(j+1)}^{(q+1)}$ and $N_{0,(j+1)}^{(q+1)}$, where q = 3, using equations (16) and (17). This loop is executed until it reaches $q_{\max}$= 3, giving $C_{(j+1)}^{(q+1)}$ and $N_{0,(j+1)}^{(q+1)}$.

CHAPTER 4

COMMUNICATION SCENARIOS

This chapter presents the models of the communication scenarios considered for the proposed iterative receiver tests, which employ pilots or no pilots.

4.1. Time-Varying Interference Model

Figure 8 shows a block diagram of a transmitter consisting of a turbo encoder, spreading, and BPSK modulation. Here, the same scenario is used as demonstrated in [4]. The roles of User (A) and User (B) are considered as the desired user and as an interferer respectively. A binary, independent and identically distributed data source from a user is the input to an encoder. A block of length m, i.e., $\mathbf{v}^{(A)} = \left[v_1^{(A)},...,v_m^{(A)}\right]$ with $v_m^{(A)} \in [1,0]$, is taken by User (A)'s encoder. Similarly, a block of length m, $\mathbf{v}^{(B)} = \left[v_1^{(B)},...,v_m^{(B)}\right]$ with $v_m^{(B)} \in [1,0]$, is taken by User (B)'s encoder. Here, only two states, i.e., "ON" and "OFF" are considered for the user's transmission. In the first test scenario, the state of User (A) is always "ON" whereas the state of User (B) is always "OFF." On the other hand, for the next test scenario, the state of User (A) is always "ON" whereas the state of User (B) changes its state periodically with a duty cycle of 10 percent.

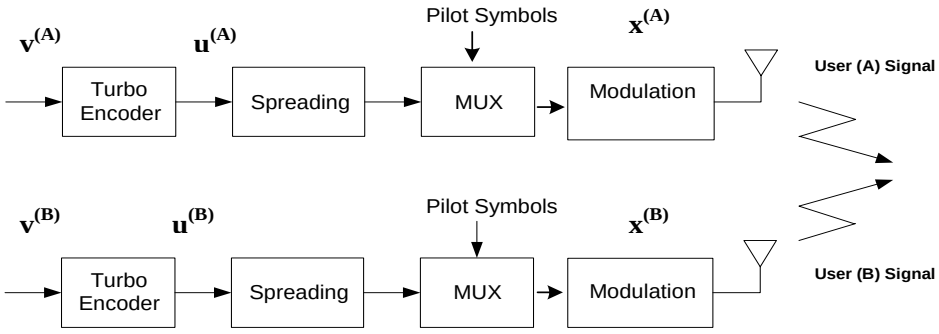

Figure 8. Time-varying interference model.

4.2 Pulse-Band Jamming Model

Figure 9 shows the power spectral density (PSD) of the pulse band signal which is partially jammed in band by the interferer. The broadband jamming energy level or PSD is $J_0=J/W$ Watts/Hz. Here, we assume that the partial-band noise jamming (PBNJ) PSD is distributed uniformly over a fraction of μW Hz where W Hz is the total system bandwidth and μ is the duty cycle. Then the jamming PSD in the jammed band is given by,

$$\sigma_J^2 = J / \mu W, 0 < \mu \le 1 \tag{27}$$

where $J = J_0 W$ is the total jamming power, and σ_J^2 is the jamming power to which the symbol is subjected with probability μ. The probability that a given transmitted symbol is not affected by the jamming power is 1-μ. In this scenario, different values of duty cycle μ are considered to see the effect of pulse jammed signal on the turbo-coded bit error rate. It is assumed that the channel is jammed by an intentional jammer whose jamming power resource is Gaussian noise.

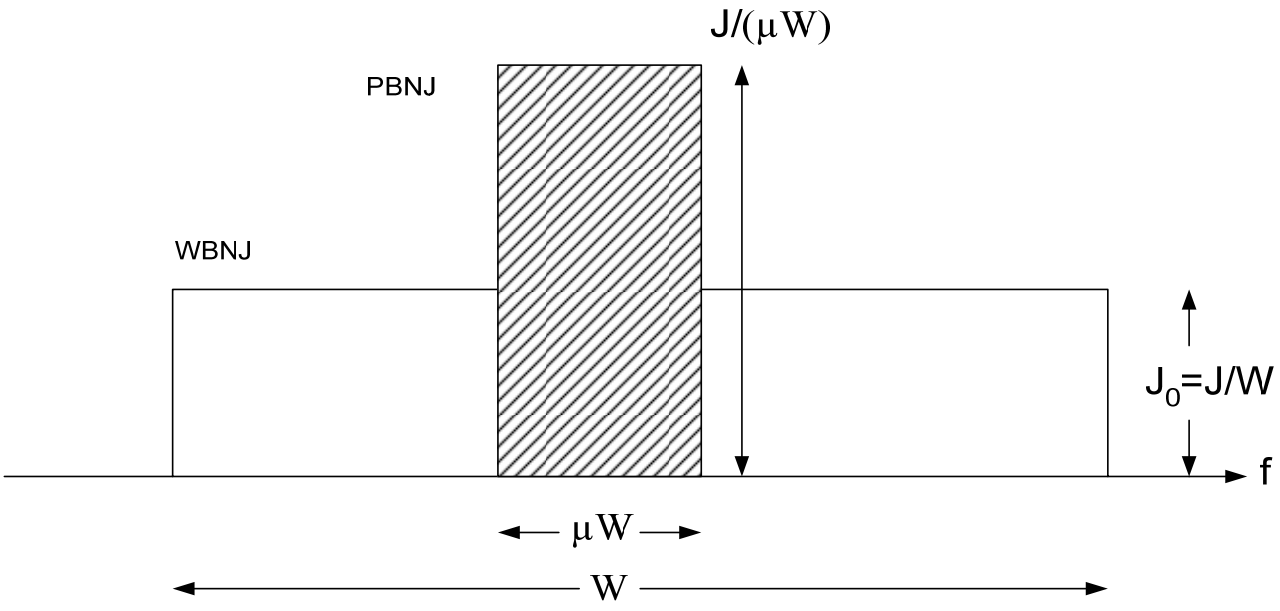

Figure 9. Pulse-band jamming model.

The BER of uncoded BPSK under PBNJ can be written as [11]

$$\overline{P}_E = (1-\mu)Q\left(\sqrt{2E_b/N_0}\right) + \mu Q\left(\sqrt{2E_b/\left(N_0 + N_J/\mu\right)}\right) \tag{28}$$

Equation (28) is used for analytical BER results for comparative purposes.

4.3 No-Pilots Case

In addition, a modified EM estimation of channel coefficients and noise PSD is proposed *without any* pilot symbols for a single-user environment excluding time-varying interference. The channel magnitude is estimated using the largest and the smallest valued received symbols per sub frame, followed by first demodulation and decoding to generate soft metrics used for refining subsequent channel estimates. The elimination of pilot symbols allows for increased energy per transmitted symbol, increased information throughput, or the inclusion of additional parity bits in general.

CHAPTER 5

SIMULATION RESULTS

This chapter discusses the performance of the proposed iterative receiver under two significant cases—*with pilots* and *without pilots.* In the first case, *with pilots*, the proposed iterative receiver was tested under two different communication scenarios such as time-varying interference and pulse band jamming. In addition, a search for the best pilot fraction is carried out under single-user environment.

In contrast to the above, the performance of the proposed iterative receiver *without any pilot symbols* is shown for single-user environment only. In addition, it also shows the significant benefits of not using pilots, such as increased energy per data symbol which is expected to compensate for any degradation in channel estimation quality compared to the pilot-symbol-aided modulation.

In the first half of this chapter, a more realistic multiuser environment is tested. The multiuser environment is tested under BPSK modulation with correlated Jakes fading, as shown in Figures 10 and 11, and uncorrelated Rayleigh fading, as shown in Figures 12 and 13. The initial receiver iteration, i.e., j = 1, is done with the aid of pilots; therefore, channel estimates $\Theta_{(j)}^{(q)} = \left(C_{(j)}^{(q)}, N_{(j)}^{(q)}\right)$ are not updated using EM iterations but obtained by simple averages in equations (16) and (17). Then, in second receiver iteration, the current estimates and the decoder feedback are used to calculate new channel estimates which are again used further to estimate improved values of $\bar{x}_{k,(j+1)}^{(q)}$ and $R_{k,(j+1)}^{(q)}$. These values are again used to calculate refined channel estimates using equations (19) and (21). The EM iterations during the j = 3 receiver iteration improved the accuracy of the decoder input.

Figure 10 shows BER versus E_b/N_0 at receiver iterations j = 1, 3, and 9 with adaptive estimation of fading coefficient and the interference plus noise PSD level. The correlated Jakes block fading model with velocity of 3km/hr is considered to generate block fading coefficients for both the users.

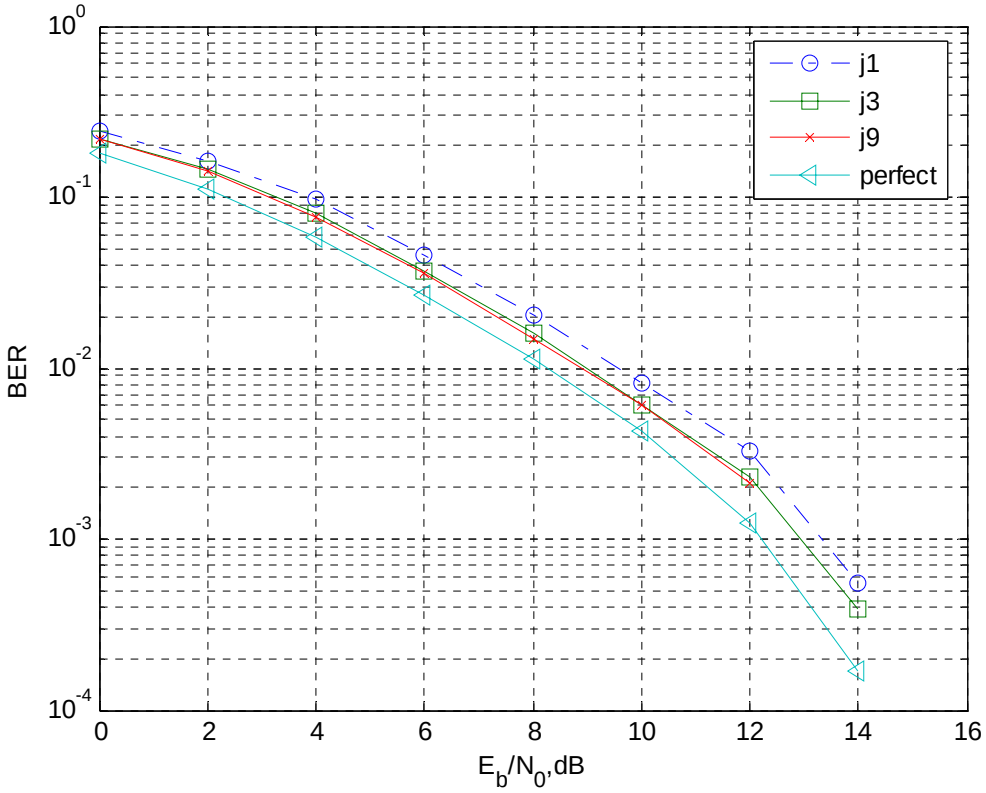

Figure 10. BER versus E_b/N_0, dB for BPSK, for codeword size 1680 and code rate R=1/3, receiver iterations j=1, 3, and 9 with adaptive PSD N_0 estimation under Jakes fading.

The duty cycle of User (B) is 10 percent, i.e., in every ten frame, the nine frames are of User (A) affected by just noise, whereas in the tenth frame, User (B) data causes an interference with the noise. The performance improvement between receiver iteration 1 and 9 is about 0.5 dB at 10^{-2} BER. It is observed that there is no significant decoding improvement between receiver iteration 3 and 9 so there is no necessary to have more receiver iterations. The difference between perfect channel coefficients and the ninth receiver estimate is about 0.8 dB.

Figure 11 shows BER versus E_b/N_0 for receiver iterations j = 1, 3, and 9 with estimating fading coefficient, and a constant of the sum of interference and noise PSD level. The environment is the same as of Figure 10. The performance improvement between non-adaptive N_0 and adaptive N_0 estimation scheme for j = 9 is 3 dB gain at 10^{-2} BER. The difference between perfect channel coefficients and the ninth iteration is about 3.3 dB.

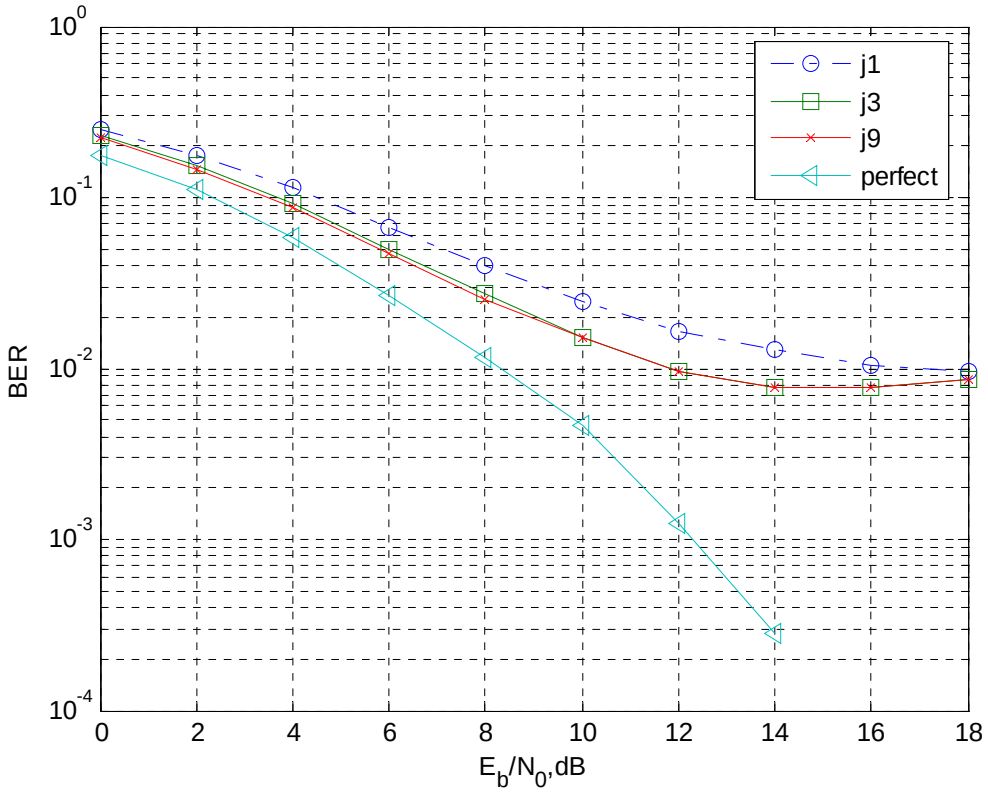

Figure 11. BER versus E_b/N_0, dB for BPSK, for codeword size 1680 and code rate R=1/3, receiver iterations j=1, 3, and 9 with non-adaptive PSD N_0 estimation under Jakes fading.

Figure 12 shows BER versus E_b/N_0 at receiver iterations j = 1, 3, and 9 with adaptive estimation of fading coefficient and the interference plus noise PSD level. Block fading coefficients for User (A) and User (B) are generated by uncorrelated Rayleigh block fading model. Here the environment is still the same as shown in Figures 10 and 11. The performance

improvement between receiver iteration 1 and 9 is about 1.3 dB at 10^{-3} BER. The gain between third and ninth receiver iteration is 0.4 dB at 10^{-4} BER. The difference between perfect channel coefficients and the ninth receiver estimate is about 0.4 dB at 10^{-5} BER.

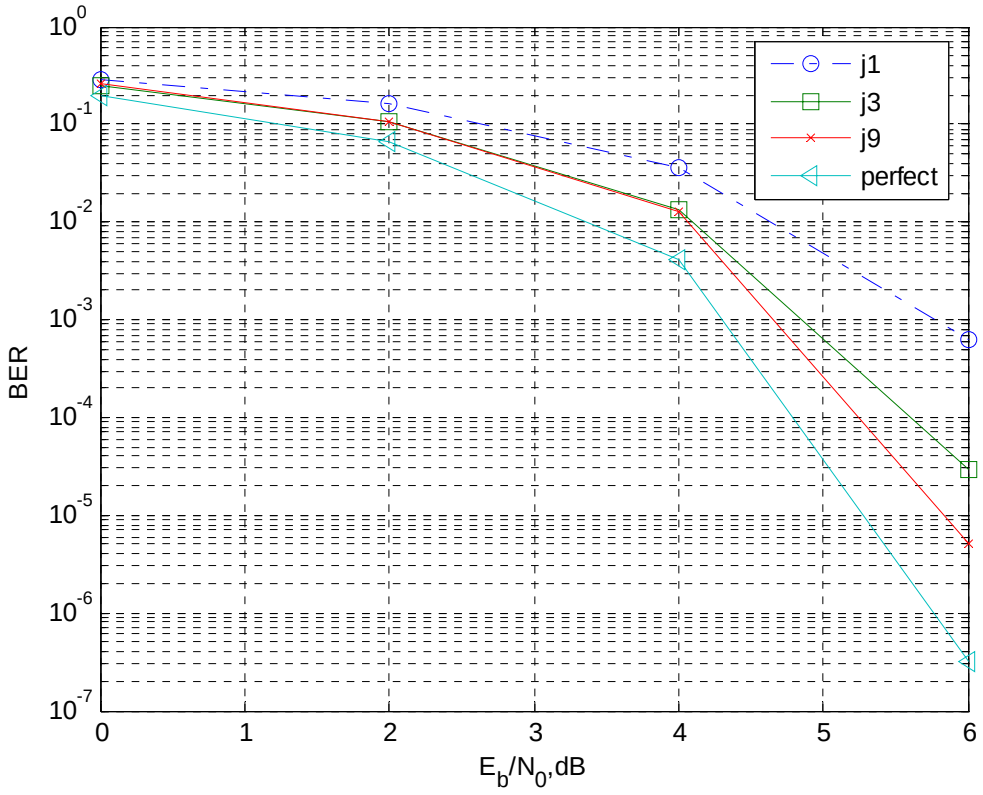

Figure 12. BER versus E_b/N_0, dB for BPSK, for codeword size 1680 and code rate R=1/3, receiver iterations j=1, 3, and 9 with adaptive PSD N_0 estimation under Rayleigh fading.

Figure 13 shows BER versus E_b/N_0 under the same environment as shown in Figure 12 for receiver iterations j = 1, 3, and 9 with only estimating fading coefficient, and keeping the interference plus noise PSD level constant, i.e., non-adaptive. The performance improvement between non-adaptive N_0 and adaptive N_0 estimation scheme for j = 9 is significant such as 6.2 dB gain at 10^{-3} BER. The difference between perfect channel coefficients and the ninth receiver estimate is about 5.5 dB at 10^{-3} BER.

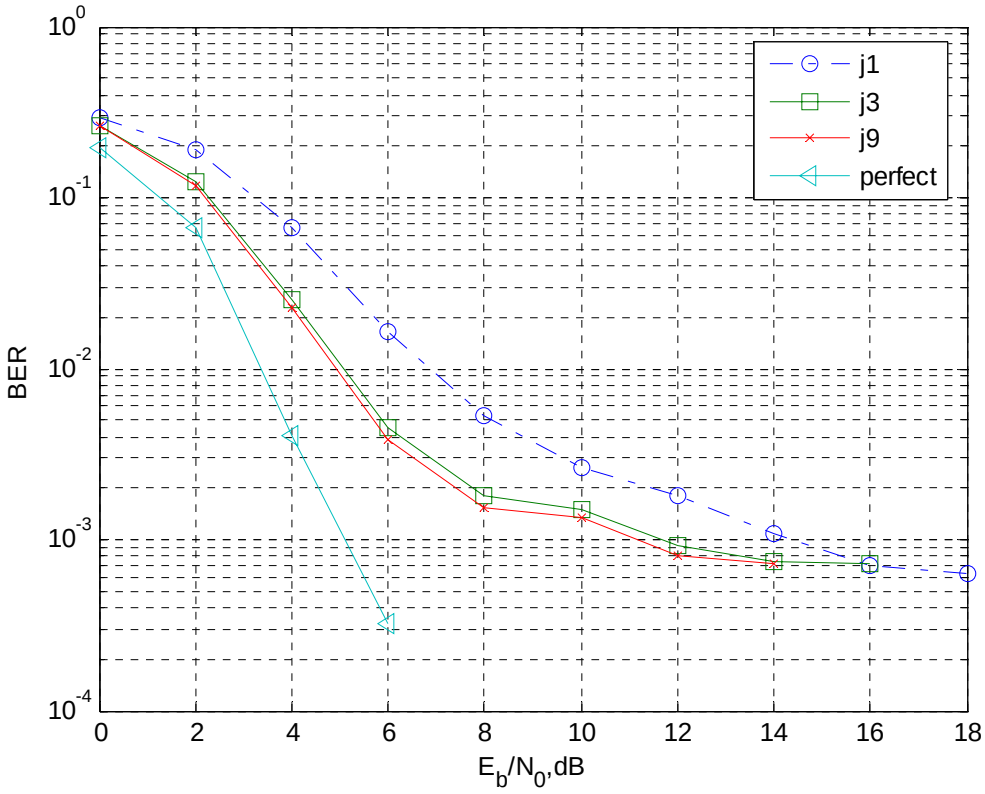

Figure 13. BER versus E_b/N_0, dB for BPSK, for codeword size 1680 and code rate R=1/3, receiver iterations j=1, 3, and 9 with non-adaptive PSD N_0 estimation under Rayleigh fading.

Figures 10 and 12 considering adaptive scheme, show the better performance than that of the non-adaptive scheme shown in Figures 11 and 13. In the adaptive scheme, when User (B) is "ON," it acts as an interferer to User (A) data, and the User (A) receiver can estimate this N_0 level change. Both the channel fading coefficients and interference PSD are estimated in the initial receiver iteration. Compared to traditional receivers where interference PSD N_0 is assumed to be constant, the decoding is more efficient which in turn gives a lower BER at the initial iteration. Thus, the adaptive scheme shows a significant gain of about 8.2dB over non-adaptive scheme at initial receiver iteration.

Figure 14 shows the BER versus E_b/N_J, where E_b/N_J is signal-to-jamming PSD ratio, for different duty cycle μ values under AWGN channel and fixed E_b/N_0=10 dB. Here, μ = 0.001,

0.01, 0.1 and 1 are considered to see the effect on the decoding performance of iterative EM turbo coded receiver under perfect channel decoding. It is observed that when μ = 1, the decoding performance of receiver is worst at the low signal-to-jamming PSD ratio. In other words, when sufficient jamming power is available, the best jamming strategy is a broad-band jamming. It is also observed that the effect of μ = 0.001 is almost constant throughout the low to higher signal-to-jamming ratio values, but BER is the worst when μ = 0.001 for E_b/N_J = 10 dB. In other words, when the available jamming power is low, the best jamming strategy is a narrowband jamming.

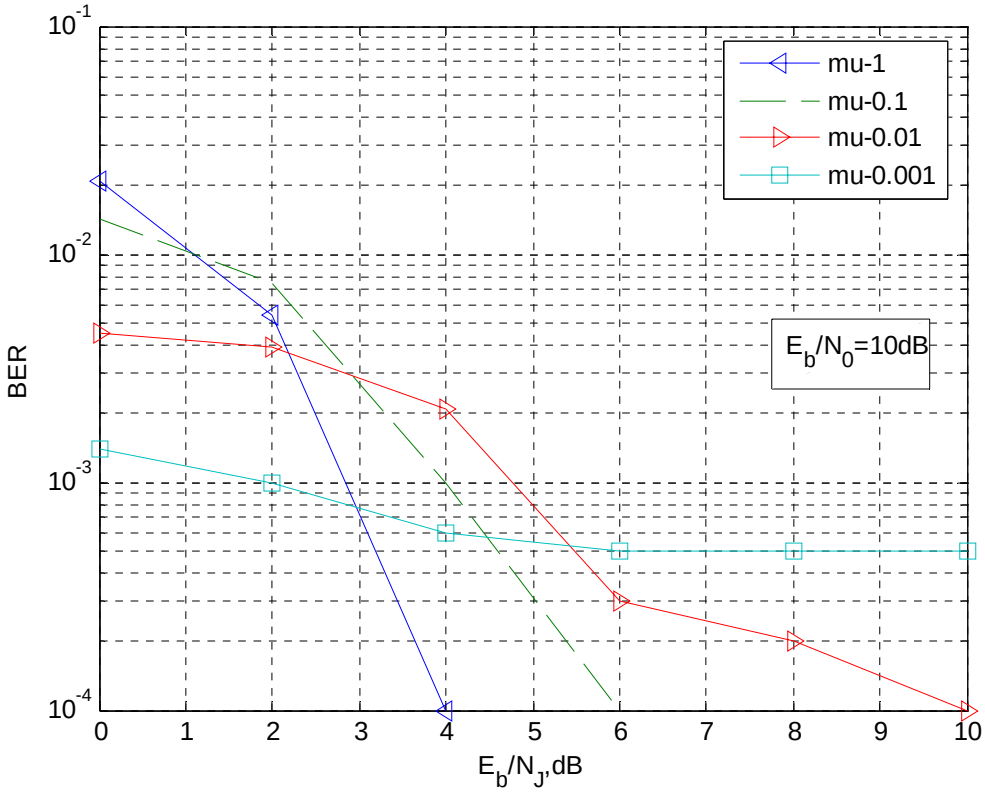

Figure 14. BER versus E_b/N_J, dB for BPSK, for 560-BS and code rate R=1/3, 3 receiver iterations, Partial Band Jamming, E_b/N_0=10dB, AWGN.

Figure 15 shows the BER versus E_b/N_J, where E_b/N_J is signal-to-jamming PSD ratio, for a duty cycle $\mu = 0.001$ under AWGN channel and fixed E_b/N_0=10 dB. It is observed that the effect of $\mu = 0.001$ is almost constant throughout the low to higher signal-to-jamming PSD ratio values. It is observed that there is 1 dB gain between the 3 EM iterations and without EM iterations at 10^{-3} BER.

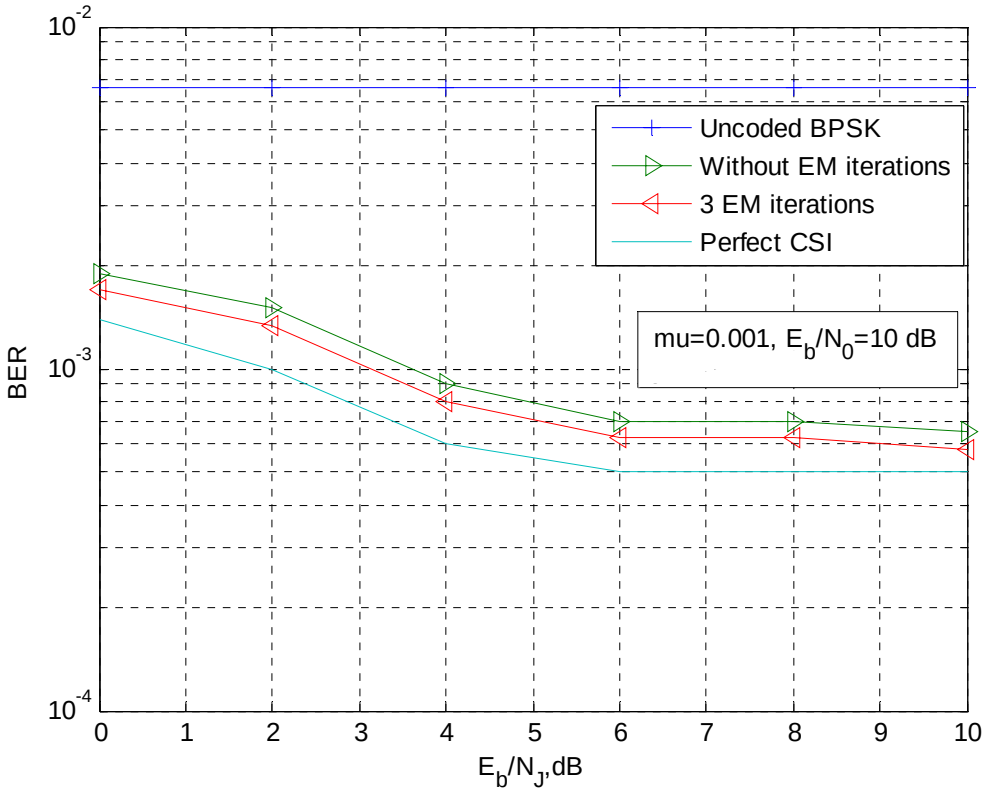

Figure 15. BER versus E_b/N_J, dB for BPSK, for 560-BS and code rate R=1/3, 3 receiver iterations, Partial Band Jamming, E_b/N_0=10dB, AWGN.

Figure 16 shows the BER versus E_b/N_J, where E_b/N_J is signal-to-jamming PSD ratio, for a duty cycle $\mu = 0.01$ under AWGN channel and fixed E_b/N_0=10 dB. It is observed that there is 0.2 dB gain between 3 EM iterations and without EM iterations at 10^{-3} BER.

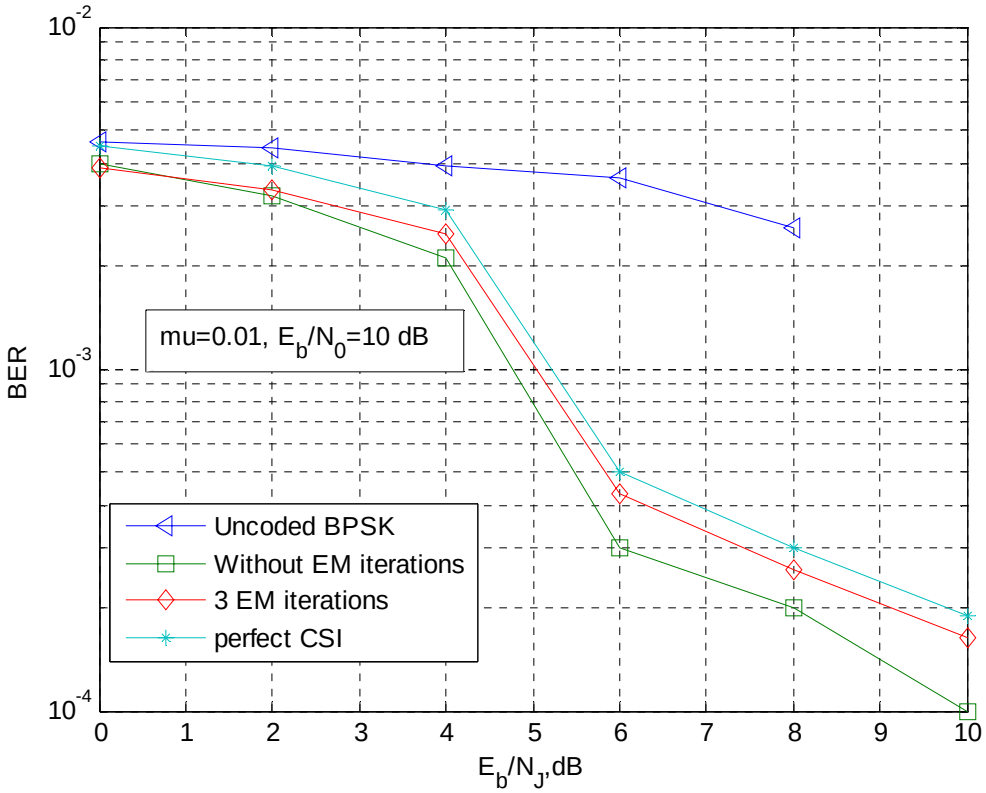

Figure 16. BER versus E_b/N_J, dB for BPSK, for 560-BS and code rate R=1/3, 3 decoder iterations, 3 receiver iterations, Partial Band Jamming, E_b/N_0=10dB, AWGN.

Figure 17 shows the BER versus E_b/N_J, where E_b/N_J is signal-to-jamming PSD ratio, for different duty cycle μ = 0.1 under AWGN channel and fixed E_b/N_0=10 dB. It is observed that there is 0.2 dB gain between 3 EM iterations and without EM iterations at 10^{-3} BER.

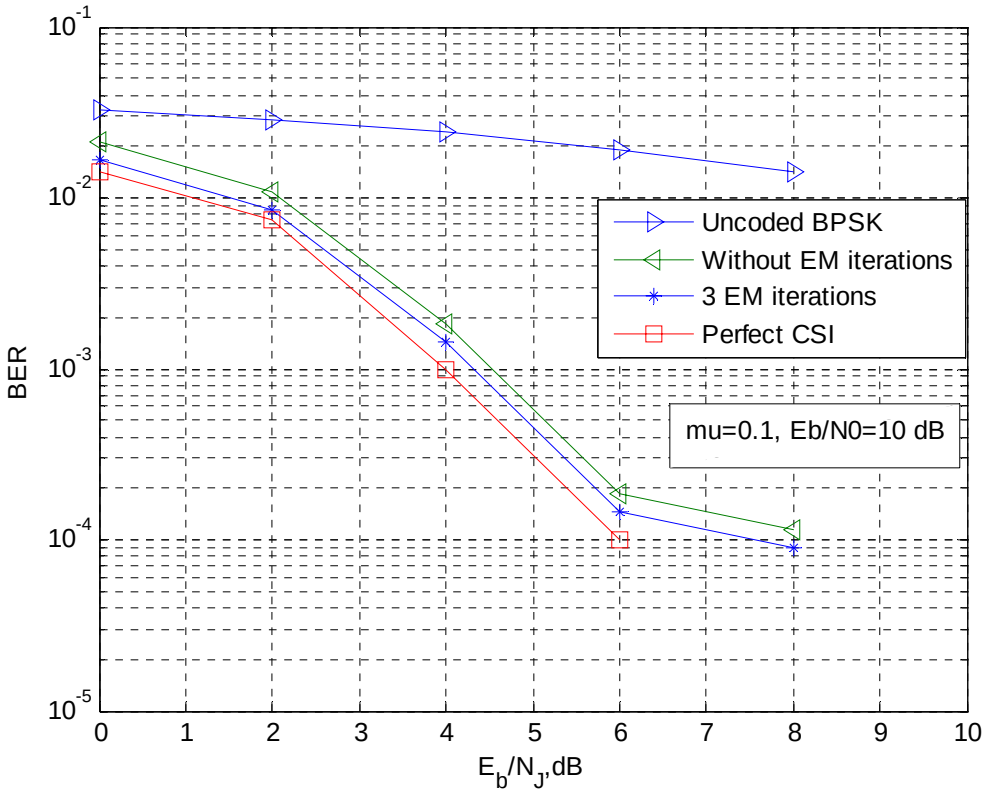

Figure 17. BER versus E_b/N_J, dB for BPSK, for 560-BS and code rate R=1/3, 3 receiver iterations, Partial Band Jamming, E_b/N_0=10dB, AWGN.

Figure 18 shows the BER versus E_b/N_J, where E_b/N_J is signal-to-jamming PSD ratio, for a duty cycle μ = 1 under AWGN channel and fixed E_b/N_0=10 dB. It is observed that when μ = 1, the decoding performance of receiver is worst at the low signal-to-jamming PSD ratio. It is observed that there is 1.2 dB gain between 3 EM iterations and without EM iteration at 10^{-3} BER.

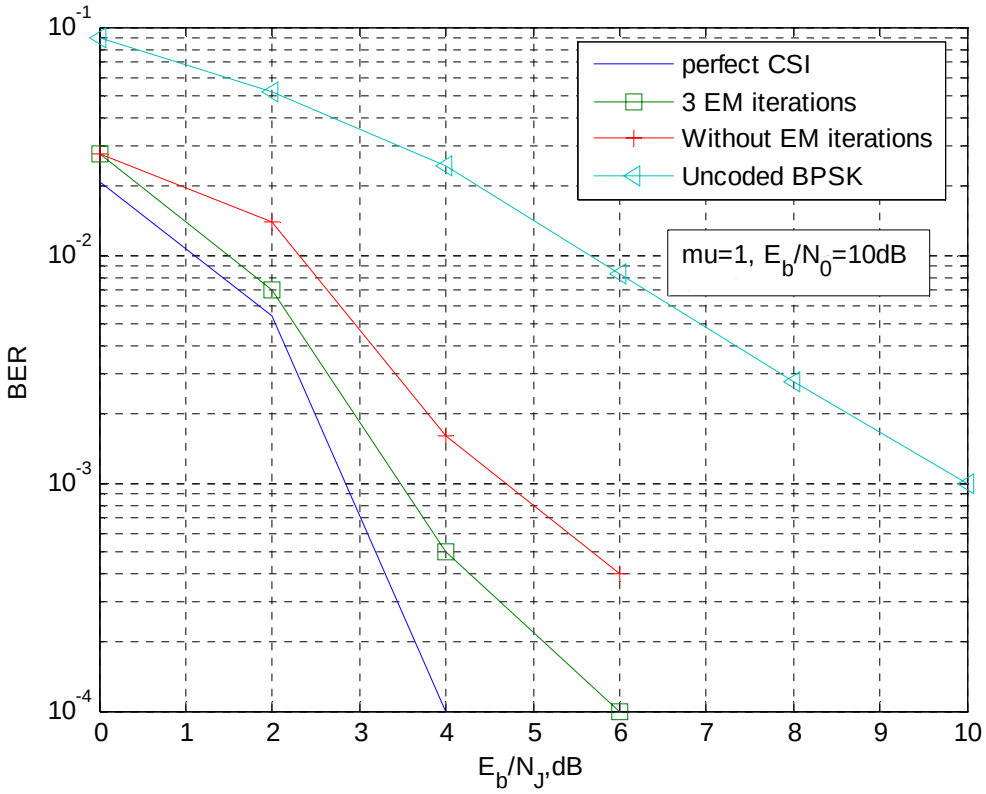

Figure 18. BER versus E_b/N_J, dB for BPSK, for 560-BS and code rate R=1/3, 3 receiver iterations, Partial Band Jamming, E_b/N_0=10dB, AWGN.

Figure 19 shows BER versus E_b/N_0 for different values of pilot fractions at 3 receiver iterations and 3 decoder iterations per receiver iteration with adaptive estimation of fading coefficient and the interference plus noise PSD level. Various values of pilot fraction such as 5%, 6.65%, 7.7%, 8.5%, 10% and 20% are considered in this extensive search for best pilot fraction in Rayleigh fading model. It is seen in Figure 19 that there is 0.5 dB gain between 8.5% and 10% pilot fractions at 10^{-3} BER.

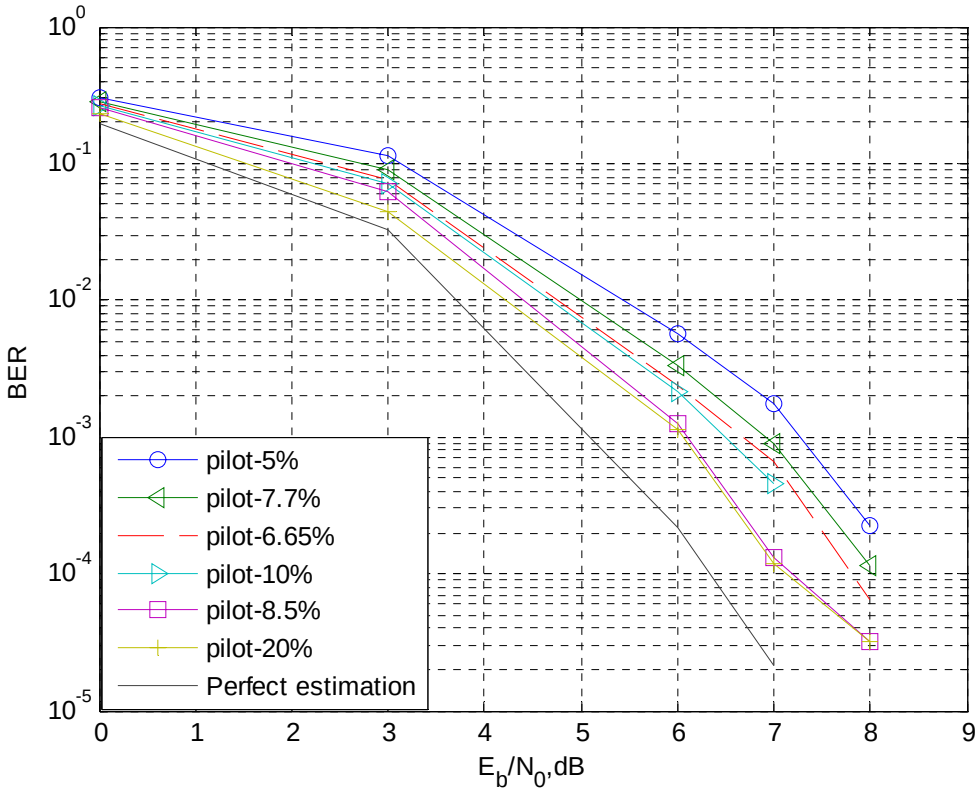

Figure 19. BER versus E_b/N_0, dB for BPSK, for codeword size 1680 and code rate R=1/3, 3 receiver iterations, search for the best pilot fraction, Rayleigh fading case.

Figure 20 shows BER versus E_b/N_0 for different values of pilot fractions at 3 receiver iterations and total 9 decoder iterations with adaptive estimation of fading coefficient and the interference plus noise PSD level in correlated Jakes fading model with velocity of 3km/hr. Various values of pilot fraction such as 6.65%, 8.5%, 10% and 20% are considered in this test of extensive search for best pilot fraction. The pilot fraction values of 8.5% and 20% show almost same performance as perfect estimation in all SNR values.

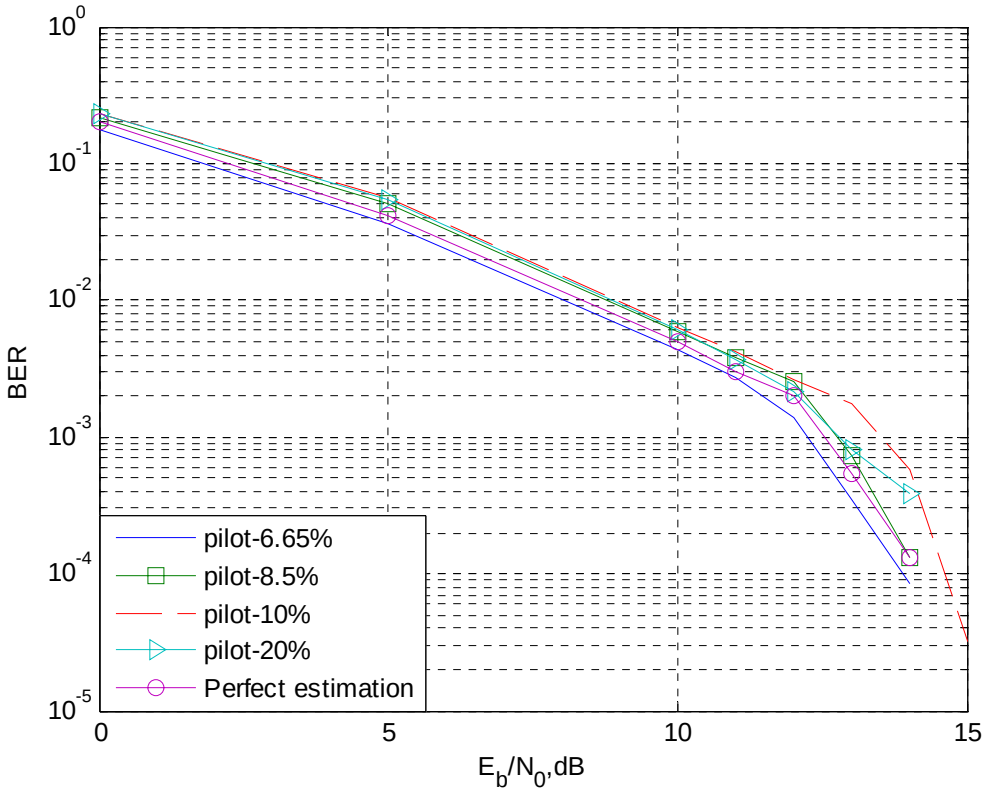

Figure 20. BER versus E_b/N_0, dB for BPSK, for codeword size 1680 and code rate R=1/3, 3 receiver iterations, Jakes fading for different pilot fractions.

Figure 21 shows the normalized *throughput* versus *pilot fraction* for fixed $E_b/N_0 = 3$ dB under Jakes fading channel. The throughput of the system is calculated using (1-BER) times (Number of transmitted information bits). The no-pilot system has a higher number of transmitted information bits than the pilot-symbol system in order to maintain a constant slot size of 752 chips as in Figure 2. For the no pilot receiver, the corresponding throughput at $E_b/N_0 = 3$ dB is seen to be higher than the throughput obtained for all pilot fractions of 5%, 6.65%, 8.5%, 10% and 20% respectively.

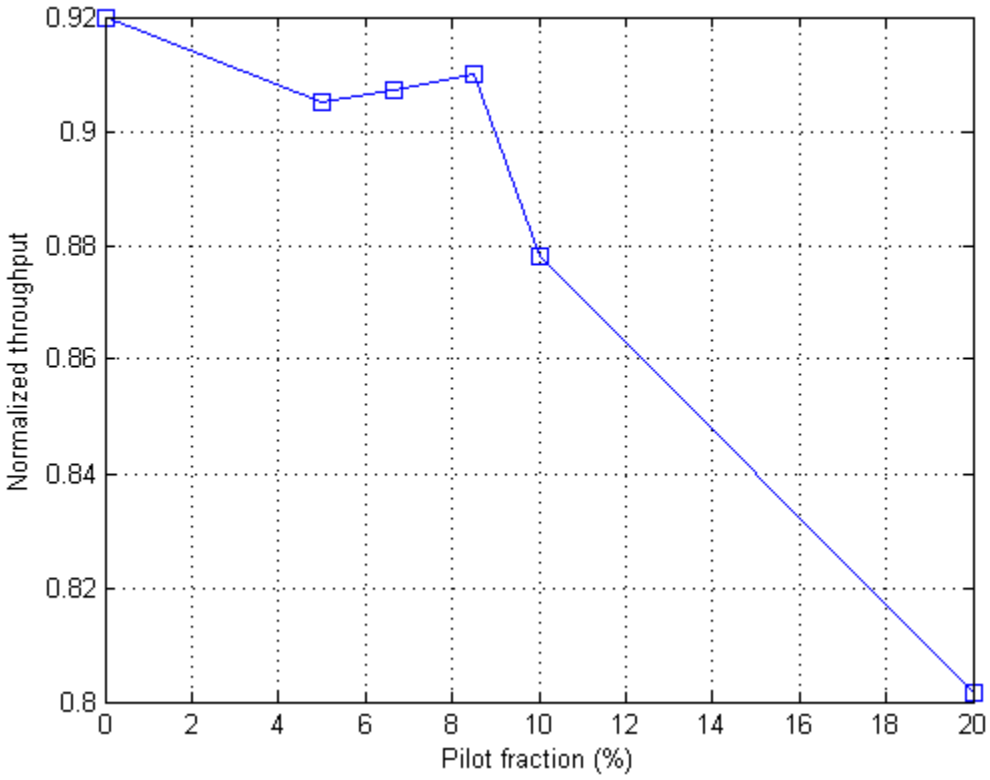

Figure 21. Throughput versus pilot fraction for fixed $E_b/N_0 = 3$ dB under Jakes Fading.

In the second half of this chapter, i.e. Figure 22, 23 and 24, no pilot case is considered. This test is done under BPSK modulation with correlated Jakes fading, as shown in Figure 22 and the uncorrelated Rayleigh fading model, as shown in Figure 23. As discussed in the iterative receiver structure section, three iterations are considered throughout the simulation. The initial receiver iteration, i.e., $j = 1$, is done by using blind estimation unlike to the previous case of pilot case. Therefore, channel estimates $\Theta_{(j)}^{(q)} = \left(C_{(j)}^{(q)}, N_{(j)}^{(q)}\right)$ are not updated using EM iterations but are obtained by rough (blind) estimation in equations (3) and (4). Then, the current value along with the decoder feedback are used to estimate new channel coefficients which is again used further to

estimate improved values of $\bar{x}_{k,(j+1)}^{(q)}$ and $R_{k,(j+1)}^{(q)}$. These values were again used to calculate refined channel estimates using equations (19) and (21).

Figure 22 shows BER versus E_b/N_0 for the no-pilot symbol, 8.5% pilot symbol, un-coded BPSK and perfect CSI cases over a Jakes fading channel with mobile velocity 3 km/hr. The difference between 8.5% pilot symbol and no-pilot symbol case at 3 receiver iterations and 3 decoder iterations is approximately 1.5 dB at 10^{-2} BER.

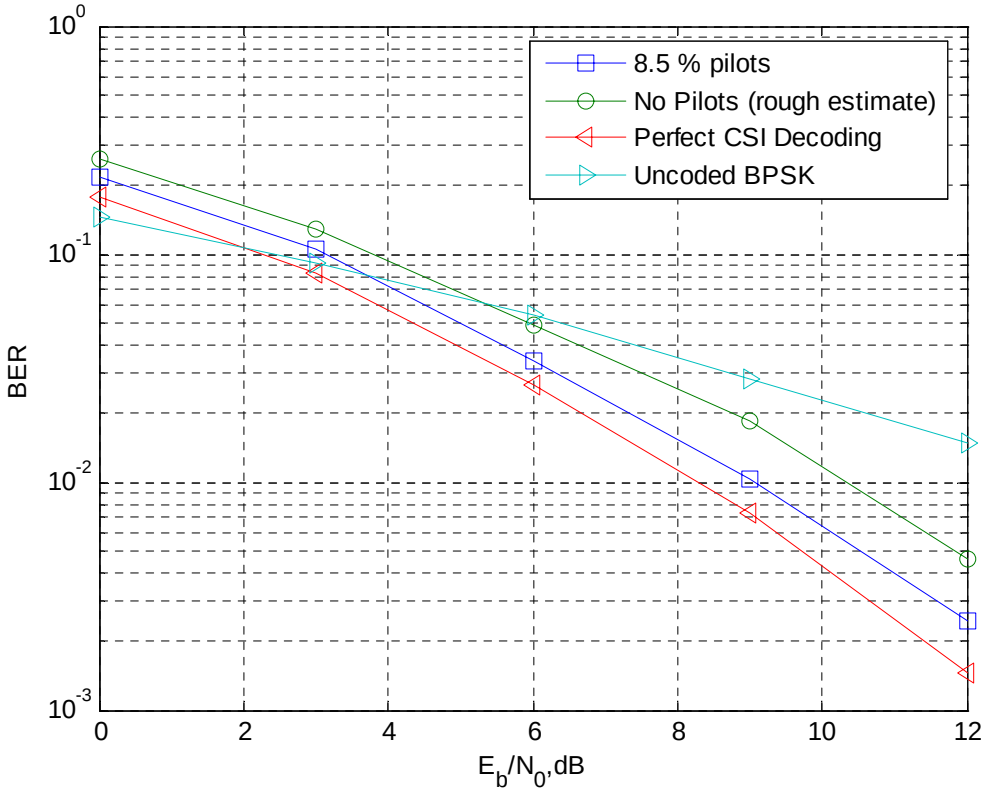

Figure 22. BER versus E_b/N_0, dB for BPSK, for codeword size 1680 and code rate R=1/3, 3 receiver iterations, for Jakes fading (v=3km/hr).

Figure 23 shows BER versus E_b/N_0 for the no-pilot symbol with EM iteration, no pilot symbol without EM iteration, 8.5% pilot symbol, un-coded BPSK and perfect CSI cases over a Rayleigh fading channel with independent fading coefficients between sub-frames. The

difference between 8.5% pilot symbol and no-pilot with EM case is 1.2 dB at 10^{-2} BER. It is also observed that the difference between no-pilot with EM and no-pilot without EM is 2.1 dB at 10^{-2} BER.

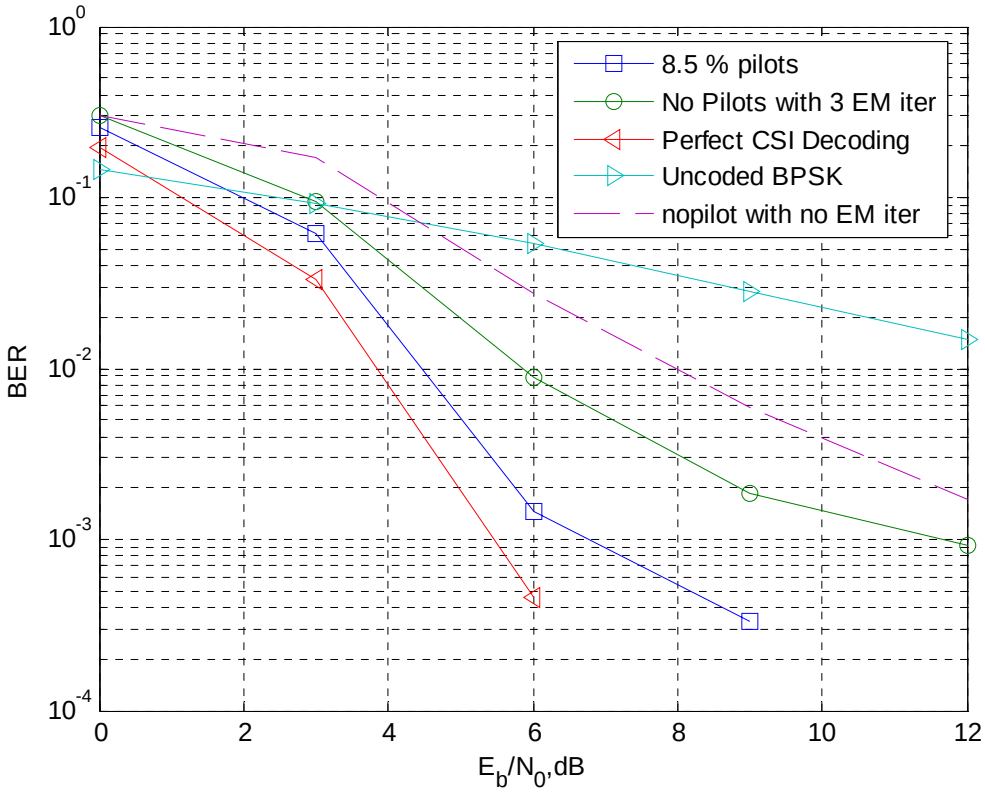

Figure 23. BER versus E_b/N_0, dB for BPSK, for codeword size 1680 and code rate R=1/3, 3 receiver iterations, for Rayleigh block fading.

Figure 24 shows BER versus E_b/N_0 for increased energy per symbol for no-pilot case, normal energy per symbol for no-pilot case, increased energy per symbol for 8.5% pilot and normal energy per symbol for 8.5% pilot cases. It is observed that the performance improvement between normal energy per symbol and increased energy per symbol for no-pilot case is 1 dB at 10^{-3} BER.

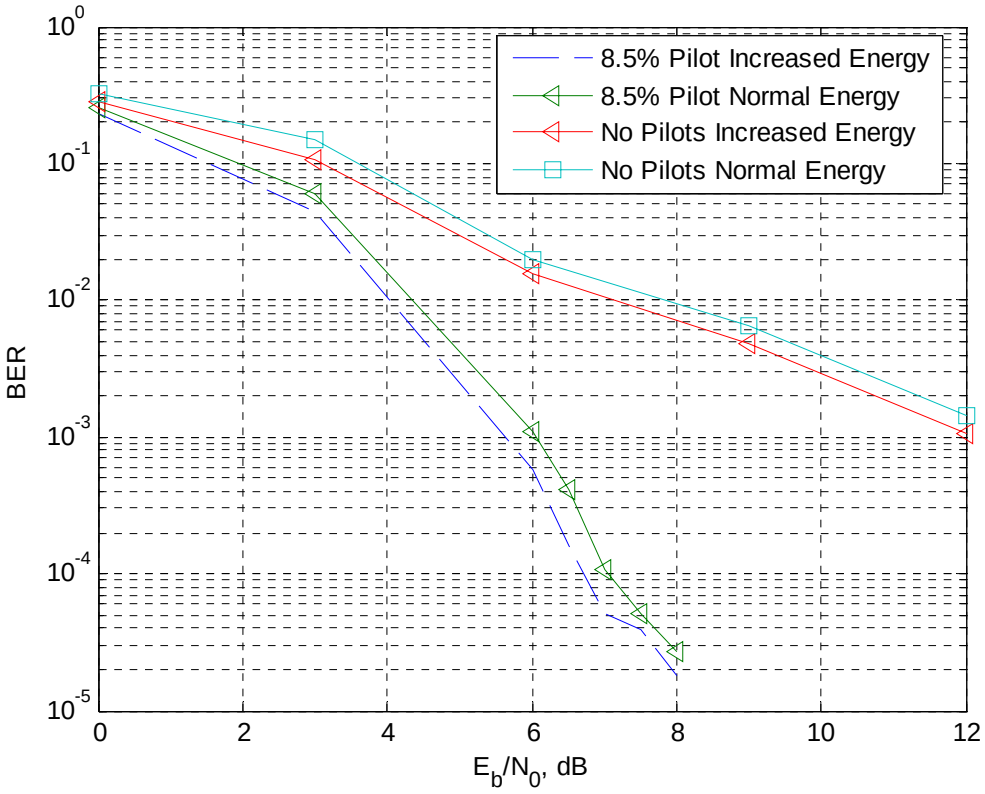

Figure 24. BER versus E_b/N_0, dB for BPSK, for codeword size 1680 and code rate R=1/3, 3 receiver iterations under Rayleigh channel fading.

CHAPTER 6

CONCLUSIONS

This thesis presents an iterative receiver with EM channel estimation using turbo codes. The performance of the proposed iterative receiver under communication scenarios, such as time-varying interference and partial band jamming are demonstrated. Two active users are considered in the time-varying interference scenario, where the desired user is always "ON" and the other user is considered as the interferer which changes its state periodically with a fixed duty cycle. The proposed receiver can adapt to a time-varying PSD scenario whereas the conventional receiver is non-adaptive to this scenario. The proposed receiver with adaptive PSD estimation scheme shows a significant gain over the conventional receiver with non-adaptive scheme.

This thesis also demonstrates an EM-based iterative turbo-coded receiver for a pulse-band jamming scenario. The proposed receiver shows the diverse effect for different values of duty cycle. The analysis is aimed at obtaining the probability of error measurement for the system under the worst case partial-band jamming. It is observed that the narrow-band jamming with duty cycle 0.001 shows the worst performance, compared to other values of the duty cycle such as 0.01 and 0.1, as well as the wide-band jamming with duty cycle 1 when E_b/N_J is high, but the wide-band jamming with duty cycle 1 is the worst when E_b/N_J is low.

This thesis also presents the EM iterative receiver for no-pilot case. The proposed receiver provides acceptable performance with no pilot overhead, thereby greatly increasing spectral efficiency or throughput compared with conventional systems. In addition, it is also observed that the elimination of pilot symbols allows for increased energy per symbol. Future work may address the application of the proposed algorithm to OFDM-based iterative receivers over frequency-selective fading channels. Additionally, the proposed no-pilot scheme may be

applied to time-varying interference scenarios such as a multi-user environment or partial-band jamming.

REFERENCES

LIST OF REFERENCES

[1] D. Torrieri, S. Cheng, and M. C. Valenti, "Turbo-NFSK: Iterative Estimation, Noncoherent Demodulation, and Decoding for Fast Fading Channels," *MILCOM 2005,* Atlantic City, New Jersey, November 17-21, 2005.

[2] D. Torrieri, E. Ustunel, H. Kwon, S. Min, and D. H. Kang, "Iterative CDMA Receiver with EM Channel Estimation and Turbo Decoding," *MILCOM 2006*, Washington D.C., October 23-25, 2006.

[3] D. Torrieri, Avinash Mathur, Amitav Mukherjee, and Hyuck M. Kwon, "Iterative LDPC CDMA Receiver with EM Estimation and Coherent Demodulation," *IEEE Asilomar* Signals, Systems, and Computers, Pacific Grove, California, October 29-November 1, 2006.

[4] D. Torrieri, Avinash Mathur, Amitav Mukherjee, and Hyuck M. Kwon, "Iterative EM Based LDPC CDMA Receiver under Time Varying Interference," *IEEE* 65th Vehicular Technology Conference VTC, Dublin, Ireland, April 22-25, 2007

[5] D. Torrieri, A. Mukherjee, and H. M. Kwon, "Iterative EM Channel Estimation for DS-CDMA Receiver Using LDPC Codes with M-ary Modulation," *in Proc. Of IEEE MILCOM*, Orlando, Florida, October 29-31, 2007.

[6] Claude Berrou and Allain Glavieux, "Near Optimum Error Correcting Coding and Decoding: Turbo Codes," *IEEE Transactions on Communications*, Vol. 44, No. 10, October 1996.

[7] Third Generation Partnership Project, Technical Specification Group Radio Access Network; "Spreading and Modulation (TDD)," 3GPP TS 25.223 V6.0.0, December 2003.

[8] Third Generation Partnership Project, Technical Specification Group Radio Access Network; "Physical Channels and Mapping of Transport Channels onto Physical Channels (TDD)," 3GPP TS 25.221 V6.0.0, December 2003.

[9] Third Generation Partnership Project, Technical Specification Group Radio Access Network; "Multiplexing and Channel Coding (TDD)," 3GPP TS 25.222, V6.0.0, December 2003.

[10] D. Torrieri, *Principles of Spread-Spectrum Communication Systems*, Boston, MA: Springer, 2005.

[11] R. L. Peterson, R. E. Ziemer and D. E. Borth, *Introduction to Spread Spectrum Communications*, Pearson Education, 1995.